iJRASET
International Journal For Research in
Applied Science and Engineering Technology

INTERNATIONAL JOURNAL FOR RESEARCH
IN APPLIED SCIENCE & ENGINEERING TECHNOLOGY

Volume: 9 Issue: VI Month of publication: June 2021

DOI: https://doi.org/10.22214/ijraset.2021.35076

International Journal for Research in Applied Science & Engineering Technology (IJRASET)
ISSN: 2321-9653; IC Value: 45.98; SJ Impact Factor: 7.429
Volume 9 Issue VI Jun 2021- Available at www.ijraset.com

Computational Investigation of through the Width Delamination of a Composite Laminate using Surface based Cohesive Contact Behaviour

K. S. Vishwanath
Assistant Professor, Department of Aerospace Engineering, IIAEM, Jain Deemed to be University, Bangalore-562112, Karnataka, India.

Abstract: The fiber reinforced polymer laminates have found extensive applications because of its advantages over other materials in terms of strength to weight ratio, manufacturing flexibility and so on. But in the transverse direction, strength is comparatively less so that a failure mechanism called delamination will occur in case of poor manufacturing or when tools are dropped. In this paper, Surface based Cohesive contact behavior is implemented at the interface between base and sub laminate to investigate for 60mm through the width buckling driven delamination growth. The computational prediction of delamination growth initiation is obtained by solving a HTA/6376C composite laminate specimen for geometric non linearity using SC8R continuum shell elements of Abaqus CAE and by plotting the inplane loads versus out of plane displacements.
Keywords: Through width delamination, Surface based cohesive contact behaviour, uniaxial compression, B-K criterion, energy release rate.

I. INTRODUCTION

The failure mechanisms of an FRP are matrix cracking, matrix debonding, delamination, kink band, micro buckling, fiber bridging and fiber pullout. And the focus of this paper is on interface delamination due to uniaxial compressive loads. Delaminations are known to lessen the overall strength and stiffness of the specimen which diminishes the load bearing ability under compressive loads. The reasons for causes of delamination are Impact, cut outs, Load generating transverse stresses, In-service loads, notch, bonded joints, Material and structural discontinuities and plydrop. Reasonably the interface is weaker in the transverse direction which will lead to high transverse and normal stresses which would induce interlaminar stresses that would lead to separation of layers. Therefore the interface is frailer compared to that of other directions of plies. Hence it is essential to predict the delamination initiation growth using damage tolerance technique [1].

II. LITERATURE SURVEY

First works were achieved by Chai et al for 1D and 2D problems [2][3]. Whitcomb and Shivakumar inspected the delamination growth due to the local buckling of a composite plate with square and rectangular embedded delaminations [1]. The buckling and post buckling behavior of debonded composite laminates were investigated by Wang and Zhang [4]. Nilsson et al investigated the delamination buckling and growth of cross ply composite panel using numerical and experimental methods and showed that for all delamination depths, the delaminated panels failed by delamination growth below the global buckling load of the undamaged panel. In addition, they found that the energy release rate of laminate is increased when global buckling mode takes place [5]. Albiol investigated the buckling and post buckling behavior of composite laminates containing embedded delamination in the composite laminate with artificial delamination. They studied the effect of various parameters on predicted response in the post buckling [6].

III. METHODOLOGY

The computation is carried out by surface based cohesive behaviour that works on the basis of traction separation relationship [7] that comprises linear elastic behaviour of normal and shear stresses at the interface defined by,

$$\mathbf{t} = \begin{Bmatrix} t_n \\ t_s \\ t_t \end{Bmatrix} = \begin{bmatrix} K_{nn} & K_{ns} & K_{nt} \\ K_{ns} & K_{ss} & K_{st} \\ K_{nt} & K_{st} & K_{tt} \end{bmatrix} \begin{Bmatrix} \delta_n \\ \delta_s \\ \delta_t \end{Bmatrix} = \mathbf{K}\boldsymbol{\delta}.$$

International Journal for Research in Applied Science & Engineering Technology (IJRASET)
ISSN: 2321-9653; IC Value: 45.98; SJ Impact Factor: 7.429
Volume 9 Issue VI Jun 2021- Available at www.ijraset.com

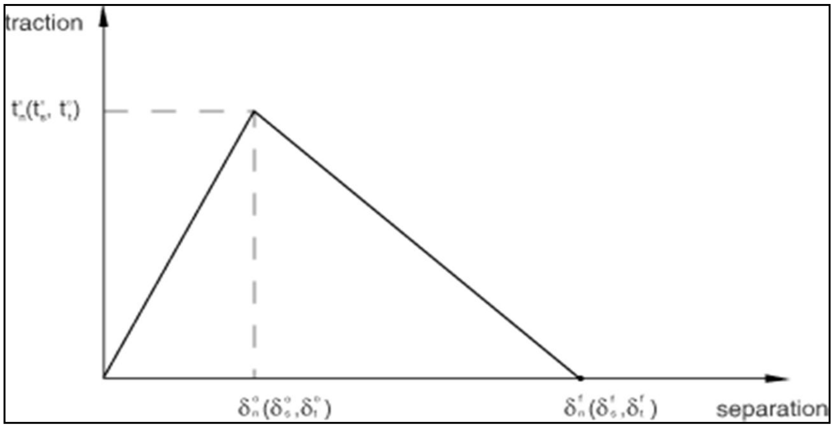

Fig 1: Cohesive surface showing Traction v separation

Where t is nominal traction stress vector and includes t_n, t_s and t_t. t_n is normal traction and t_s, t_t are the shear tractions. In addition, the corresponding separations are denoted by δ_n, δ_s and δ_t. The cohesive contact behavior comprises 2 phases; they are damage initiation and damage evolution. Basically damage initiation occurs when the cohesive behavior (as shown in the figure 1) at a point in the contact domain starts degrading which is captured by quadratic stress criterion given by

$$(\langle t_n \rangle / t_{no})^2 + (t_s/t_{so})^2 + (t_t/t_{to})^2 = 1$$

Where t_{no}, t_{so}, t_{to} represents the values of the highest contact stress (traction). The damage evolution law shows the cohesive stiffness degradation. Fig.1 shows the cohesive law for single loading. A scalar damage variable, *D*, represents the damage at the contact point given in [7] as

$$D = \frac{\delta_m^f(\delta_m^{max} - \delta_m^0)}{\delta_m^{max}(\delta_m^f - \delta_m^0)}$$

which δ_m^{max} refers to the maximum value of the effective separation, δ_{mf} is the effective separation at complete failure and δ_{mo} is relative to the effective separation at the initiation of damage. The constitutive response of Fig. 1 can be written as

$t = K_p\delta \quad \delta < \delta_o$

$t = (1-D)K_p\delta \quad \delta_o \le \delta \le \delta_f$

$t = 0 \quad \delta \ge \delta_f$

For delamination growth initiation, B-K criterion is applied [9].

In real time problems, delamination growth occurs due to energy release rates in all 3 directions namely normal and 2 shear directions. Hence total energy release rate is given by $G_T = G_I + G_{II} + G_{III}$ and the nodes open up and the damage propagates when the condition $G_T/G_C \ge 1$ is satisfied, where critical energy release rate is found by B-K criterion that has contribution from all 3 modes given by $G_C = G_{IC} + (G_{IIC} - G_{IC})(G_S/G_T)^{\eta}$, where $G_S = G_{II} + G_{III}$.

Now a HTA/6376C composite laminate specimen having stacking sequence of [90/(0/90)3//(0/90)14] is considered as in [6]. The symbol // shows pre-delamination location in the material. The geometry of specimen with single delamination is shown in the Fig. 1. The material properties of HTA/6376C composite plate are E_{11}=131 GPa, $E_{22}=E_{33}$= 11.7 GPa, $G_{12}=G_{13}$=5.2 GPa, G_{23} =3.9 GPa, $\nu_{12} = \nu_{13}$ =0.3, ν_{23}=0.5, N=30 MPa, S=T=30MPa, G_I^C= 260 (J/m2) and $G_{II}^C = G_{III}^C$=1025(J/m^2). The total thickness of the laminate is h=4.5mm as shown in the Fig 2.

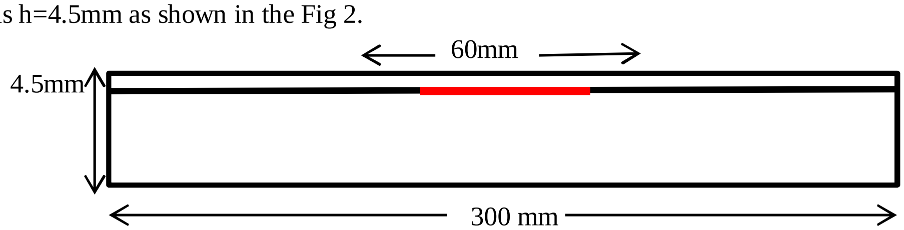

Fig 2: Illustration of the specimen

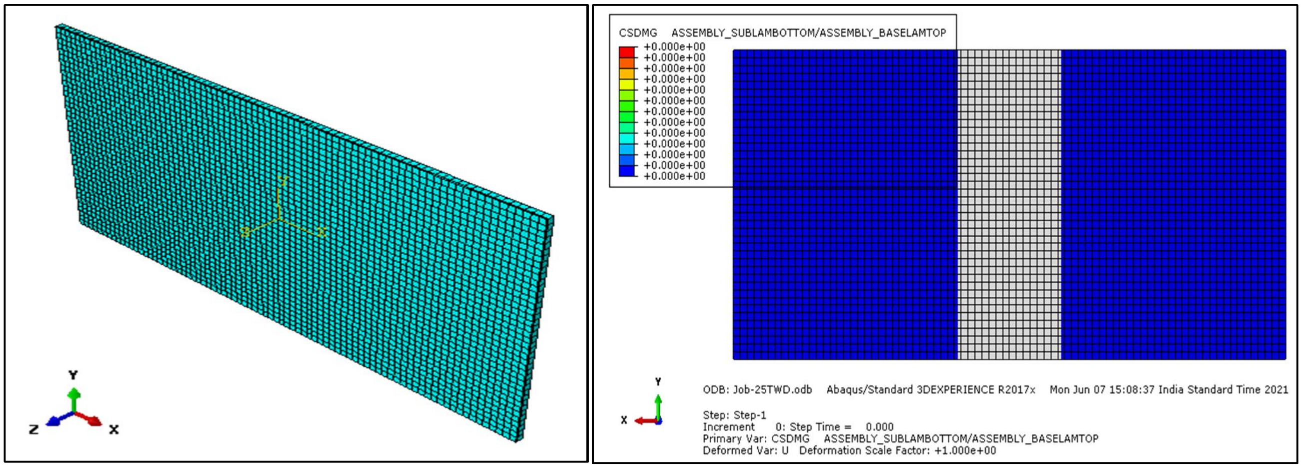

Fig 3: Meshed plate and initial delamination geometry

The above Fig 3 shows the meshed plate and initial delamination geometry of the specimen whose boundary conditions are u1=u2=u3=0 on the left extreme side, and u2=u3= 0 on the right side with a compressive load of u1=2mm compressive load is applied for the first step in terms of displacement. And for the second step, 5mm is applied.

IV. RESULTS AND DISCUSSION

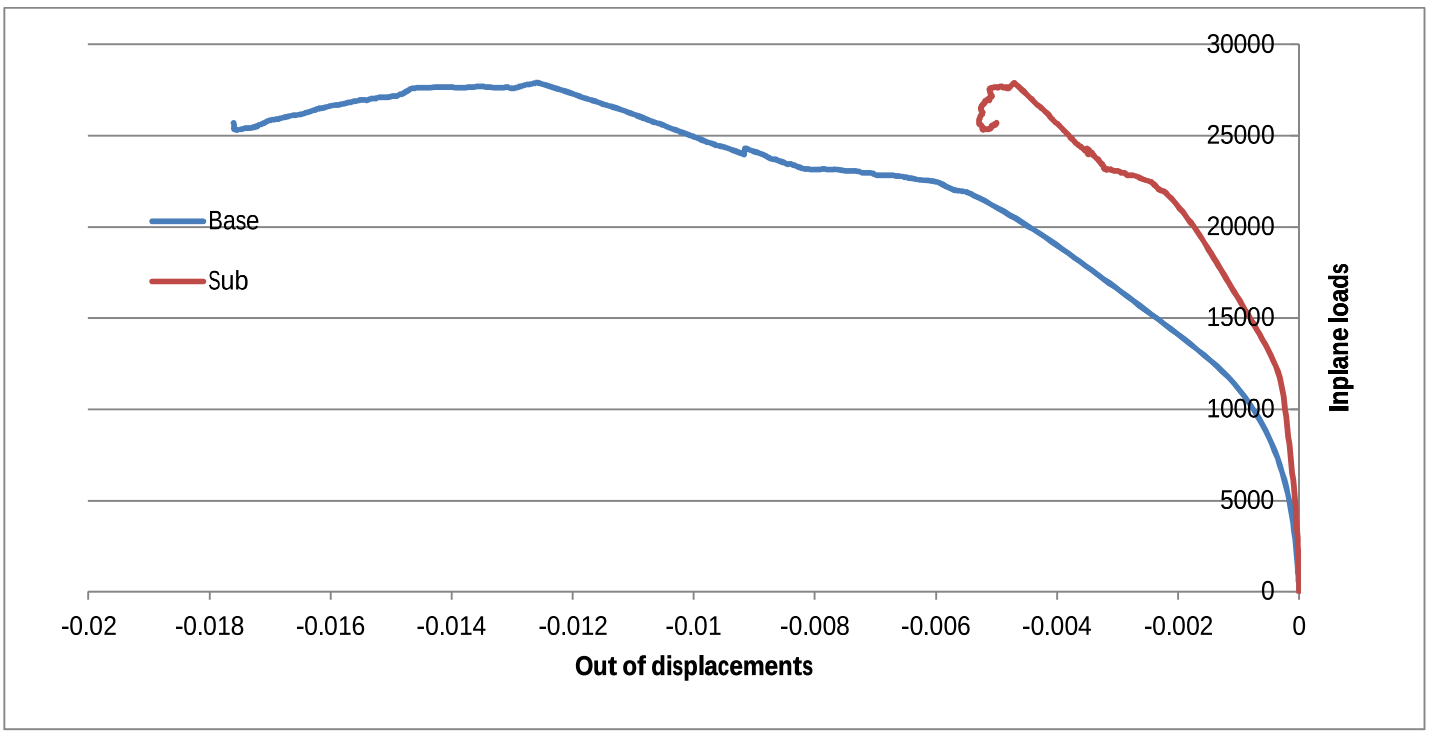

Fig 4: Inplane loads vs Out of plane displacements

Inplane loads at the left support versus out of plane displacements at the centre of the base and sublaminate is plotted as shown in Fig 4. From the plot it can be clearly observed that Local buckling can be observed at 2.3KN. The initial post-buckling response is ruled by the buckling of the thinner sub-laminate alone which is known as thin-film buckling. Postbuckling behaviour can be either stable or unstable. In this analysis, stable post-buckling and local buckling occurs at 2.3KN after the delamination growth initiation, later the shape changes to an opening mode shape occurs at 27.9KN. And afterwards slowly the laminate collapses much later.

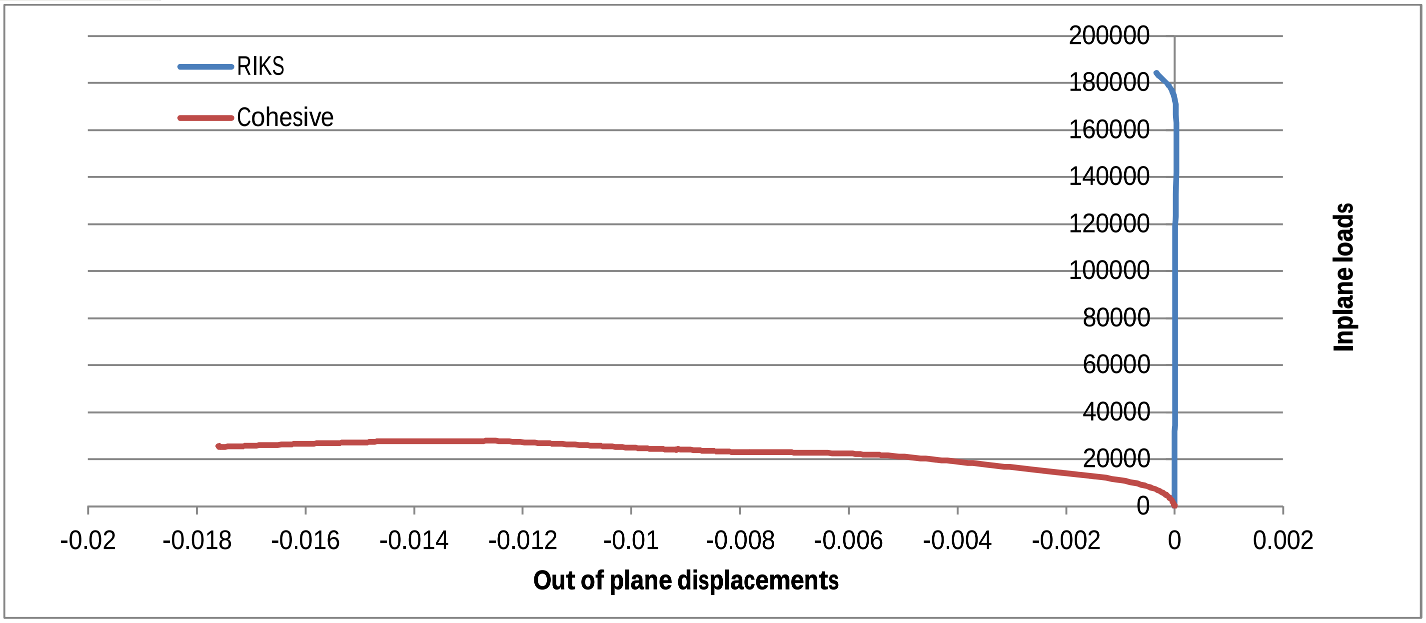

Fig 5: Inplane loads vs Out of plane displacement

Fig 5 shows plot of inplane loads versus out of plane displacement of the specimen considered in this paper by RIKS method and Delamination using surface based cohesive contact method. It is clear that the overall load carrying capability has reduced considerably which is about 27.9KN because the analysis is not carried until collapse and is stopped much earlier right after opening mode shape occurs.

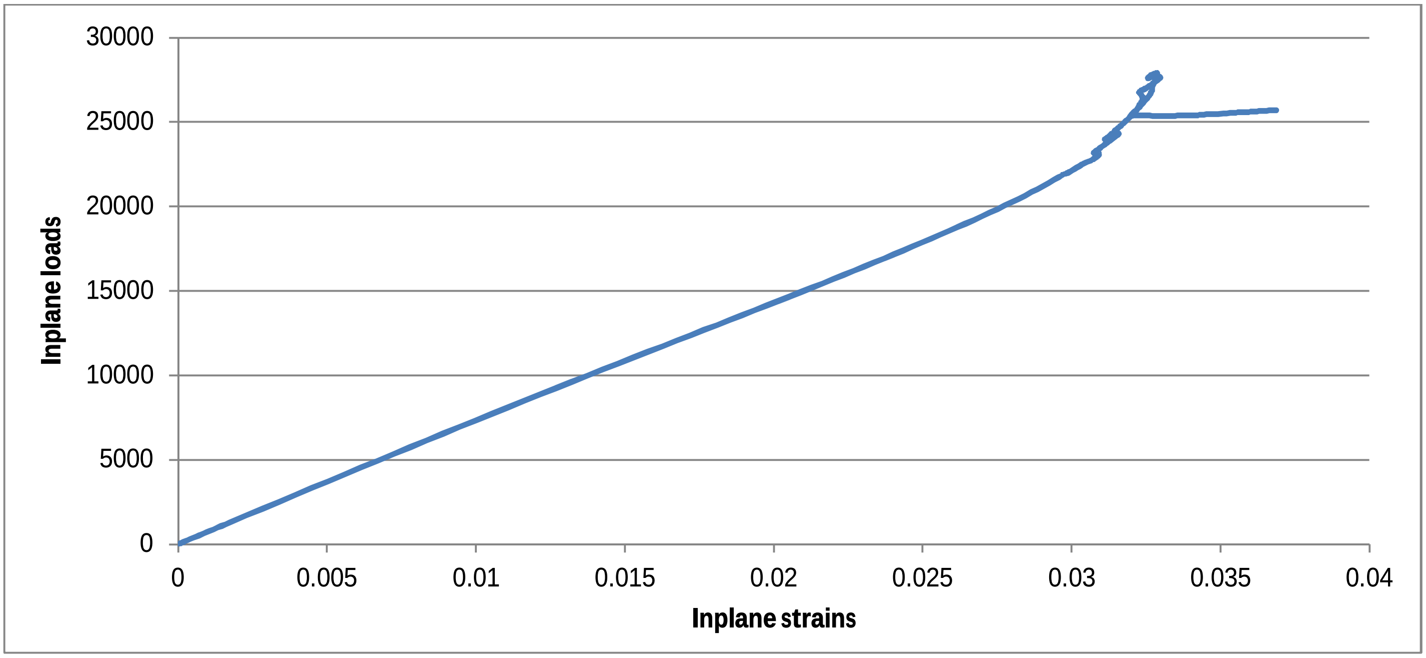

Fig 6: Inplane loads vs Inplane strains

The above Fig 6 shows the behavior of the specimen in which inplane loads versus inplane strains is plotted in which local buckling can be clearly seen at 2.3KN followed by opening mode shape at 27.9KN.

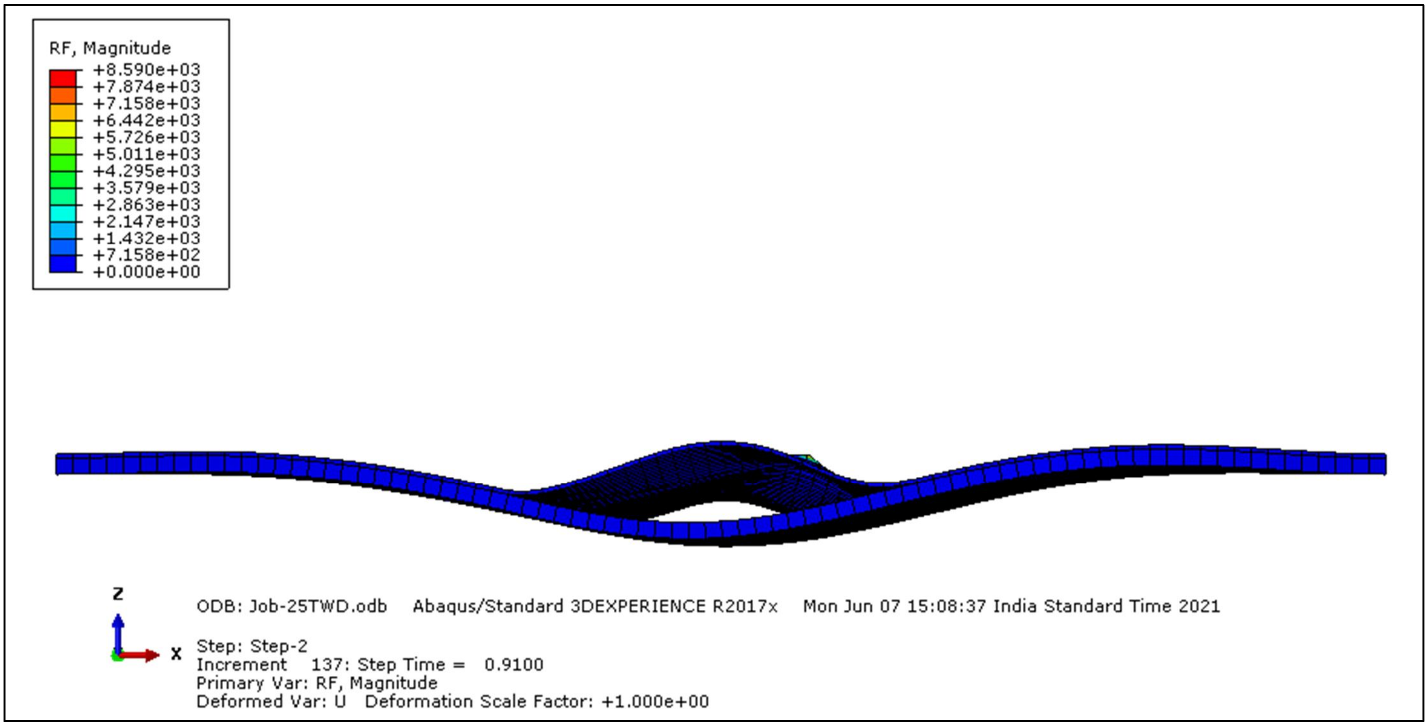

Fig 7: Contour plot of reaction force in the direction of applied loads

Fig 7 shows the opening mode shape of the laminate after the analysis is completed.

V. CONCLUSION

In this paper a specimen considered from [8] is analyzed computationally using surface based cohesive behaviour in ABAQUS CAE. From the analysis, buckling, post buckling using both RIKS and surface based cohesive behaviour has been observed and compared for reduction in load carrying capacity followed by damage evolution and the transitions made by base and sub laminates so that local buckling, opening mode delamination were observed.

VI. ACKNOWLEDGEMENT

I thank my family and almighty for everything.

REFERENCES

[1] Whitcomb JD, Shivakumar KN. Strain-energy release rate analysis of plates with postbuckled delaminations. J Compos Mater 1989;23:714–34.
[2] Chai H, Babcock CA, Knauss WG (1981),"One dimensional modelling of failure in laminated plates by delamination buckling", Int J Solids Struct.17(11):1069–83.
[3] Chai H, Babcock C (1985). Two-dimensional modelling of compressive failure in delaminated laminates. J Compos Mater. 19:67–98.
[4] Zhang Y, Wang S., Buckling, post-buckling and delamination propagation in debonded composite laminates part2: numerical application, Journal of Composite Structure. Vol. 88, 2009, pp.131–46.
[5] Hossein Hosseini-Toudeshky, Samira Hosseini, Bijan Mohammadi., Delamination buckling growth in laminated composites using layerwise-interface element, Vol. 92, No. 8, 2010 ,pp. 1846-1856.
[6] Albiol D., Buckling analyses of composite laminated panels with delamination, *Master's Thesis*, University of Politecnico di Milano, 2010
[7] Dassault Systemes Simulia. Abaqus 6.14. Analysis User's manual, Vol.5.
[8] Tashkinov, M. A., Modelling of fracture processes in laminate composite plates with embedded delamination Frattura ed Integrità Strutturale, 39 (2017) 248-262.

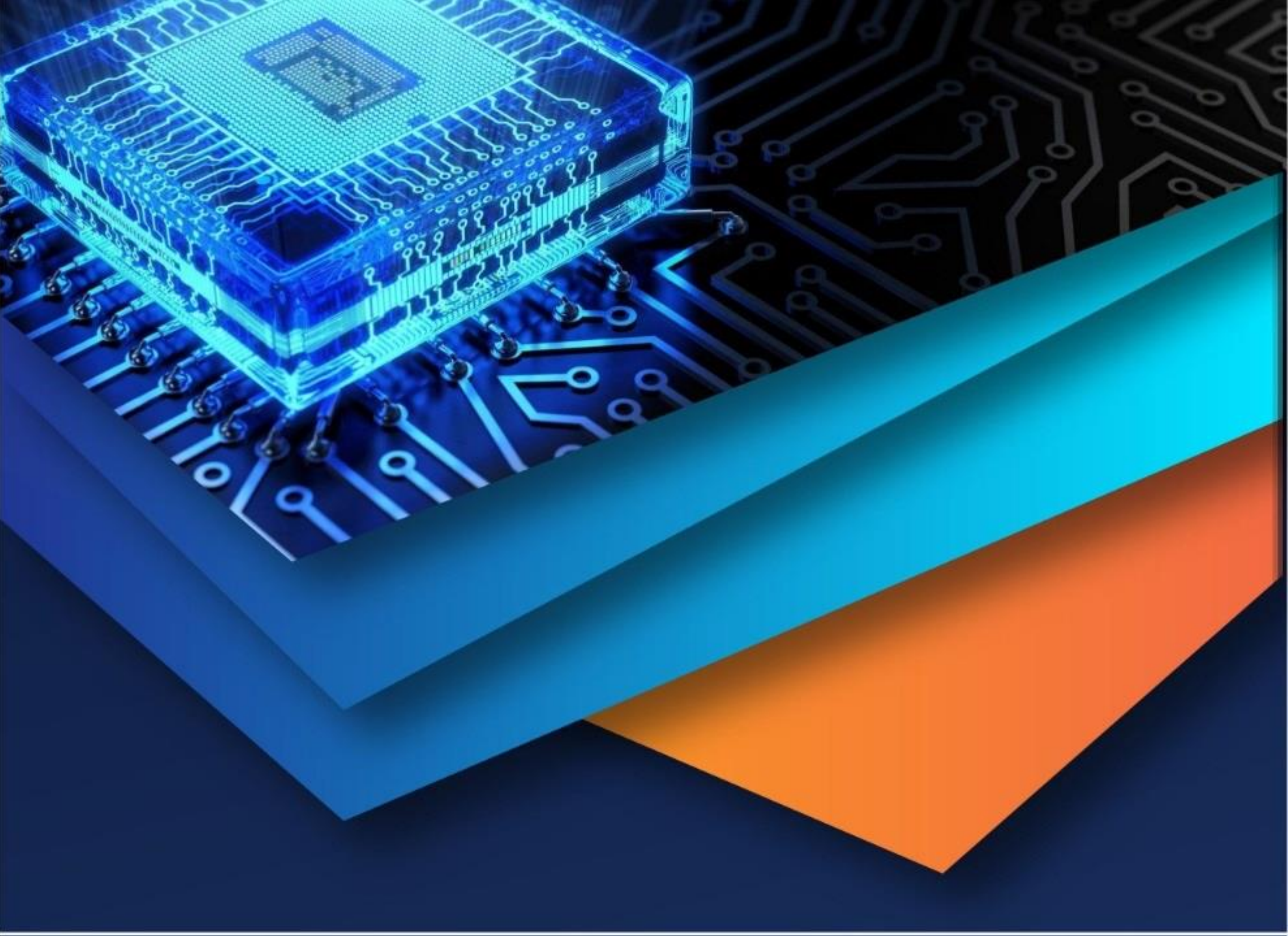

10.22214/IJRASET

INDEX COPERNICUS

45.98

ISRA JIF

IMPACT FACTOR: 7.129

TOGETHER WE REACH THE GOAL

IMPACT FACTOR: 7.429

ISI

INTERNATIONAL JOURNAL FOR RESEARCH

IN APPLIED SCIENCE & ENGINEERING TECHNOLOGY